Failure Cause Analysis of a 5 KW Wind Turbine Blade in Extreme Wind Conditions

TEODOR MILOS[1], ILARE BORDEASU[1*], RODICA BADARAU[1], ADRIAN BEJ[1], DORIN BORDEASU[2]
[1]Politehnica University of Timisoara, 2 Piata Victoriei, 300006 Timisoara, Romania
[2] VIA University College, Horsens, Denmark

The paper presents a case study on the causes that led to the breaking of the blades on a 5 kW wind turbine due to high wind loads at a wind speed of 30 m/s . The paper is structured in two parts. In the first part there are presented the functional design and material aspects essential for a blade proper operation, with an analysis of the critical areas where the breaking of the blade was initiated. There are also analyzed the causes the materials prescribed in the technical design and the manufacturing technology failed upon a short time wind gust of up to 30m/s. In the second part of the paper there are presented corrective technical solutions for materials and blade shape design in order to ensure a higher mechanical strength of the blade suitable for a safe and reliable operation for the specific environmental conditions. The studies and the solutions considered for the blade design improvement shown in the present paper are based on finite element analysis (FEA) as well as on blade static tests performed by using distributed sandbag loads.

Keywords: wind turbine, blade, wind speed, GFRP, Finite Element Analysis, load, stress

Small power wind turbines with fixed rotor blades (fixed blade pitch angle) must be equipped with protection systems in order to withstand extreme wind speeds [2], [6]. This protection system is usually either a centrifugal mechanism that rotates the blades toward the feathered position when the rotational speed exceeds a certain allowed limit, or a furling system that turn the rotor out of the wind direction. The last one is performed either by tilting up the rotor by the means of the trust force, or by rotating the turbine over the tower axis due to the imbalance between the moments developed by the trust force upon the rotor, which is eccentrically setoff to the tower axis, and respectively the aerodynamic force upon the yaw wind vane. In some cases an ultimate level of protection is provided by electrical or mechanical braking which brings the rotor in the stop position. The protection system automatic reaction is not instantaneous, there is a transitional period, and finally when the wind turbine is brought in the protection position or the rotor is braked, the blades remain further exposed to wind. In order to face these strong winds (wind speed of over 25m/s) the rotor and the blades in particular must be designed and sized to withstand the aerodynamic forces developed by those extreme winds. This requirement completes the design/ verification requirements considered for material mechanical strength to fatigue loading. According to the IEC standards [9] the safety coefficients assumed for design verification must be selected between 3 and 10 according with the operational regime and the type of loads (i.e. static or variable).

Rotor blade design characteristics and materials

The wind turbine rated parameters [1], [2] are as follows:

Rotor power: 5500 W
Rotor diameter: 7 m
Maximum blade tip speed: 45 m/s
Maximum rotational speed: 120 rpm (150 rpm can be accidentally achieved)
Rotor swept area: 38 m^2
Tip speed ratio: 3...4
Rotor power coefficient (maximum expected values): 0.428...0.466
Solidity : 0.122
Rated wind speeds (associated to 5.5 kW rotor power , 120 rpm operational speed, assuming an air density of 1.1 to 1.5 kg/m^3) : 8 ... 8.7 m/s

The 3D contour of the blade has been generated by using three types of NACA laminar airfoils (i.e. NACA 65_2 – 415; NACA 65_3 – 418;NACA 65_4 – 421) [4], the blade tip having a 200 mm winglet attached to it (fig. 1a).

The outside layer of the blade (blade shell) having a thickness of 5...10 mm, is made of fiber glass reinforced polyester (FGRP) [7], [8], manufactured by hand lay-up in successive layers in a mold. It comprises of two shell halves (inner and outer) which finally are glued on the outline including a reinforcement metal insertion in the blade root section, too (fig.1b), [5]. The gap between the two halves of the blade shell is filled with polyurethane foam aiming to reduce the vibration and to increase the blade stiffness.

Case study on the blade damages

The wind turbine designed and operated by "Politehnica" University of Timisoara encountered on March 19, 2013 a severe damage. Under a strong wind gust of about 30 m/s and due to an initial exfoliation occurred on one blade, followed then by a strong mechanical imbalance of the rotor, the three blades broke away from the rotor hub.

Further on it is given a brief analysis of the damages caused on the three blades.

Findings from the online recording

The online recording and the step by step analysis of the recorded sequences revealed that due to the high wind speed (about 30 m/s), one of the blades being partially unbound and having cracks on its tip area, greatly bent

* *email: ilarica59@gmail.com*

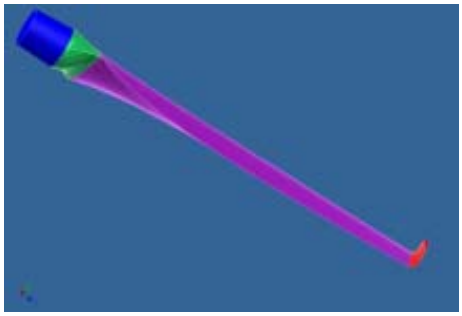

a) 3D wind turbine blade model with a 200mm winglet [4]

b) metallic reinforcement in the blade root section

Fig. 1. Wind turbine blade with fastening and reinforcing components

a

b

c

Fig. 2. Pictures of wind turbine after the incident a) lateral view; b) front view ; c) zoom on the impact zone

hitting the tower and getting stripped off on the contour where it was glued; the inner shell torn away and in the next sequence hit the next blade following in the rotational direction. The shock caused the breaking of the blade shaft, which split from the rotor. Strongly unbalanced the rotor induced a rotation with large amplitude oscillations in all directions which led to breaking off the shaft of the third blade.

Findings and pictures from the site

Images captured on the site (fig. 2) reveal visible bold marks done through impact over the tower's conical section by the blade winglet which caused the rotor damage. At the same level there are paint scratches caused by the tangential touching after the blade broke off.

Findings on the broken blades

By analyzing all the three blades it was found that the last blade was affected by the breaking shock only in the tip area, due to the impact with the blade already broken in the first phase of the incident (fig. 3). Although it did not show substantial damages, the shaft flange of 50 mm thick, shown in figure 3, was broken off showing the magnitude of the shock.

Figure 4 shows the damages of the first broken blade, which were increased when hitting the ground

The study of the damaged blades shows that the FGRP shell in the metallic reinforcing insertion area, withstood without any cracking or breaking. However, according to our design marks and by analyzing the recorded video, the first blade detached from the rotor and torn off in two (i.e. inner and outer part) due to the binding failure (fig. 4). In this figure it can be seen that the polyurethane foam did not had uniform adhesion allover the surface of each of the two shells. We consider that the damage of the FGRP structure of the blade that touched the tower was caused by elastic deformations with large blade deflections,

Fig. 3 The least damaged blade on the shell, but having the shaft broken

Fig. 4. Broken blade

exceeding those recorded during the static tests performed in-house at the blade manufacturer [7]. It is also possible that during the static tests the blade FGRP structure could have been weakened, or some cracking areas were initiated within the binding line of the shell halves. The

Table 1
MATERIAL PROPERTIES [8]

Name	FGRP (Fiber Glass Reinforced Polyester)	
General	Mass Density	1,85 g/cm^3
	Yield Strength	49,6 MPa
	Ultimate Tensile Strength	360 MPa
Stress	Young's Modulus	20,52 GPa
	Poisson's Ratio	0,253 ul
	Shear Modulus	8,18835 GPa
Stress Thermal	Expansion Coefficient	0,000005 ul/c
	Thermal Conductivity	0,3 W/(m K)
	Specific Heat	750 J/(kg c)

breaking of the two flanges of the blade shafts was caused through the impact with the tower, which generated unexpected loads not considered in the turbine design stage, and consequently overloaded the shaft. The reason for this is that after the first failure the unbalanced rotor masses developed additional loads, including vibrations over the emergency braking threshold.

Finite element analysis (FEA) of the loading status for the damaged blade

Finite element analysis (FEA) method is one of the modern computing tools used for Strength of Materials. The advantage of this numerical (or digital) method is the availability to refine the meshing structure (e.g. mesh), reducing the elements where inconclusive areas, or even instability areas could occur. Another major advantage is that the method is quite similar regardless the shape or the size of the object subject to loading. The method graphically presents the model colored gradually from blue to red through green and yellow, with the convention that the red spectrum points out the most loaded areas. Thus, the loading status and the critical zones are instantly visualized, which allows to take further actions to dimensionally optimize the analyzed object. Additionally, there is also an option to generate an animation of the loads.

Blade 3D model generation

In order to manufacture the two molds for the blade shells, a 3D virtual model of the blade was generated in a CAD/CAM system and then used on a 5 axis CNC cutting machine to get the blade negative. Keeping the blade exterior surface geometry, the blade shape was generated as a hollow 3D model. This is the outer layer from FGRP with a 5mm thickness. Toward the blade root section, within the part with metal insertion, the FGRP layer thickness gradually increases to 10mm according to the blade design. The inner core of the blade, made of polyurethane foam, with the geometric shape of the blade inside gap, was neglected as strength contribution because it has a very low mechanical strength, having actually only the role to damp the vibrations. For this blade model used for FEA the metal insertion was not included, looking to find specifically the evolution of the loading within the composite material without any contribution of the metal insertion, although this is obviously essential for the blade root as was proven and revealed by the incident reported in the present paper. The shape of the airfoils, their coaxial setting, pitch angles and the radial position were strictly respected according to the 3D model given initially through the technical project of the blade [5].

Specific characteristics of FGRP considered for blade design

For FGRP it was assumed an orthotropic material having the following properties [8] (table 1).

Constraints and loads applied on the blade 3D model

The induced stresses into the blade GFRP structure were evaluated assuming that the 3D blade is embedded in its fastening section on the rotor hub. The blade was loaded on the inner half shell with a distributed force, equivalent with the air flow dynamic pressure acting upon the blade windward side when rotor is frontally exposed to wind.

Dynamic pressure, on the inner part, was determined as:

$$\Delta p = C_x \rho \frac{v^2}{2} \quad (1)$$

The input data used for FEA corresponds to the extreme conditions:

- Air density: $\rho = 1.5$ kg/m^3 (cold and dry air)
- Aerodynamic drag coefficient $C_x = 2$ (flat plate exposed perpendicularly to the air flow direction)
- Considered wind speed: $v = 30$ m/s = 108 km/h

With these data results that $\Delta p = 1350$ Pa

This pressure was successively applied on the inner side of each 200 mm long blade element.

Domain mesh

FEA meshing has as starting point the surface elements of the parts considered for being analyzed. For a better definition of the blade sections, consisting of NACA airfoils, it was applied a distributed meshing on the airfoil outline on at least 50 points, with gradually increasing density from the trailing edge toward the leading edge. On this local mesh, it was then generated the FEA solver global mesh. The image of the resulted FEA mesh is shown in figure 5.

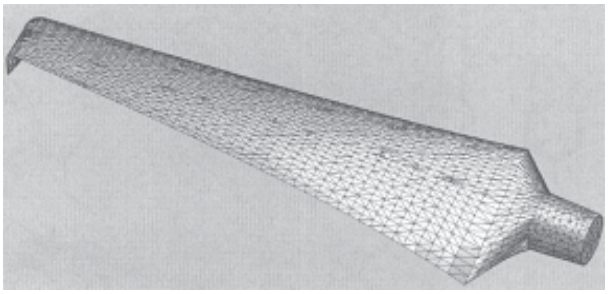

Fig. 5. Blade mesh

Interpretation of the FEA results

The distributed pressure load applied upon the blade generates in the embedded section of the blade root a shear force F and a bending moment M, each comprising three components regarding the three reference directions, respectively X, Y, Z, as given in table 2.

Figures 9 to 15 show the displacement and stresses produced by the pressure load upon the blade, with their minimum and maximum values . These are as follows:

Constraint Name	Reaction Force		Reaction Moment	
	Magnitude	Component (X,Y,Z)	Magnitude	Component (X,Y,Z)
Fixed Constraint:1	2249.56 N	-2176.15 N	3581.32 N m	-691.008 N m
		-569.949 N		3511.25 N m
		-3.28082 N		-139.781 N m

Table 2
REACTION FORCE AND MOMENT ON CONSTRAINTS

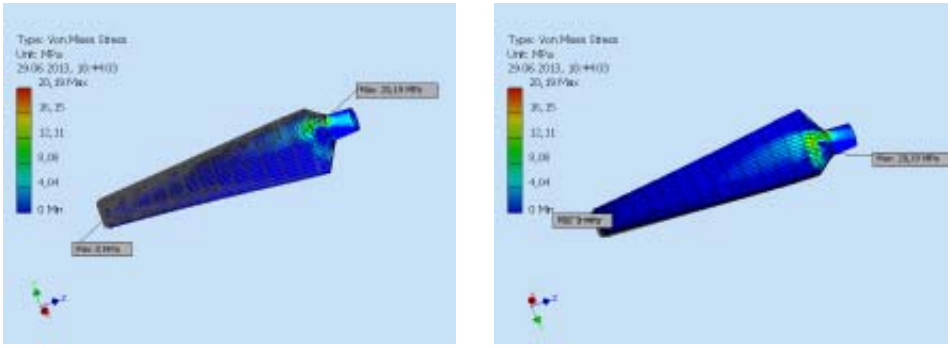

Fig. 6. Von Mises Stress distribution

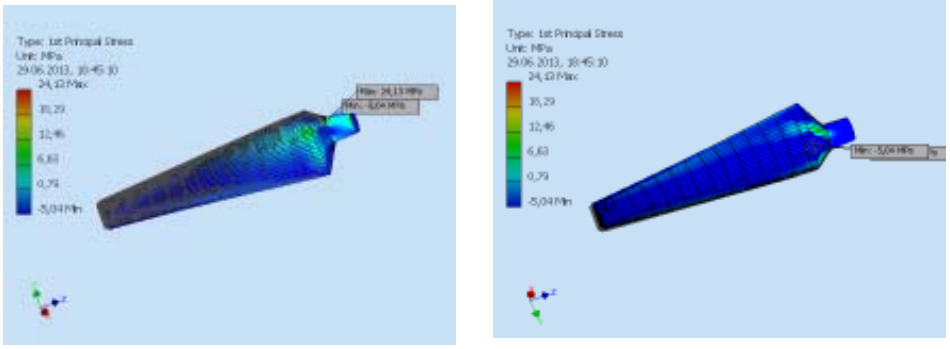

Fig. 7. 1st Principal Stress distribution

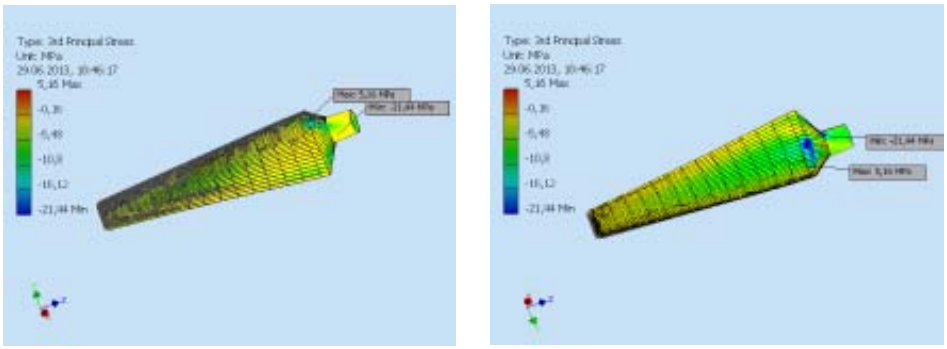

Fig. 8. 3rd Principal Stress distribution

• Figure 6 gives the variation of Von Mises Stress - which represents the summation of the longitudinal and tangential stresses based on Von Mises Stress Method. The maximum values are located in the transitional area from the circular section to the airfoil shaped section. The presence of the reinforcing metal insertion in this area greatly reduces the loads in the GFPR structure. The maximum stress values does not exceed the allowable yield strength of 49.6 MP associated with the assumed blade GFRP material;

• Figure 7 shows the variation of tensile (compression) stress. The maximum values occur approximately in the same area as Von Mises Stress does. Here it can be also noted that the stress values do not exceed the allowable yield strength of 49.6 MPa;

• Figure 8 shows the variation of the shear stress. Maximum values appear in the blade root sections, on the leading edge. It is also notable that the allowable yield strength of the GFRP material of 49.6 MPa is not exceeded;

• Figure 9 shows that the maximum displacement of 17.47 mm produced at the tip of the blade, opposite to the root section, has acceptable values placed into the range of those specified within the blade technical design;

• Figure 10 provides data referring the safety factor values , ranging between 2.46 and 15 regarding the yield strength limit. It can be noted that the minimum value is associated to the same area where the Von Mises Stress gives the maximum value, and revealing consequently the connection between these two parameters . Also, the minimum value shows that the most stressed section requires to be reinforced;

• Figure 11 shows that the maximum displacement are on X axis direction, the direction from which the wind blows and acts normal on the blade surface, causing the elastic deformation, which caused the impact between the winglet and the tower.

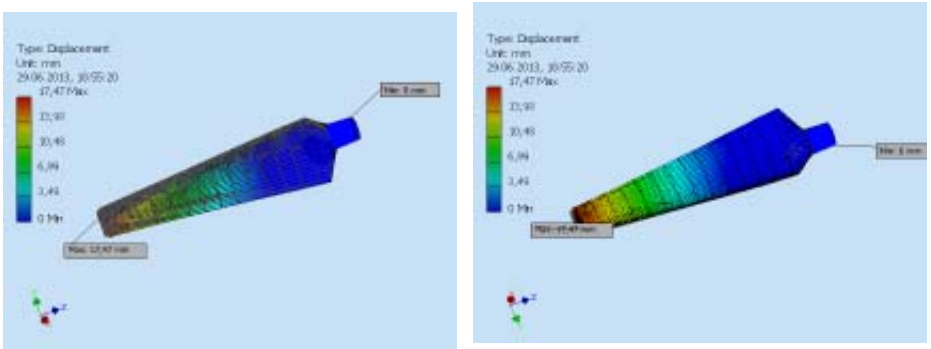

Fig. 9. Displacement distribution

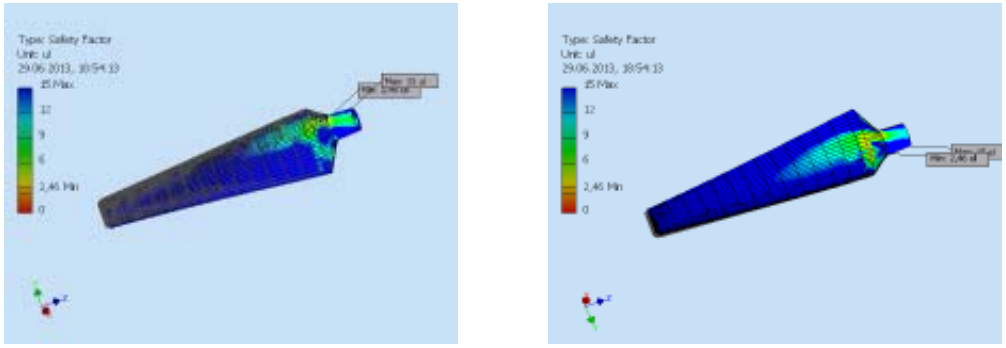

Fig. 10. Safety Factor distribution

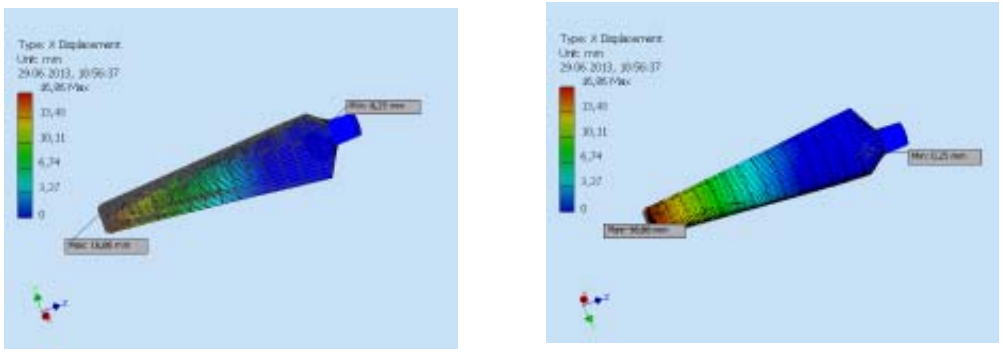

Fig. 11. X Displacement distribution

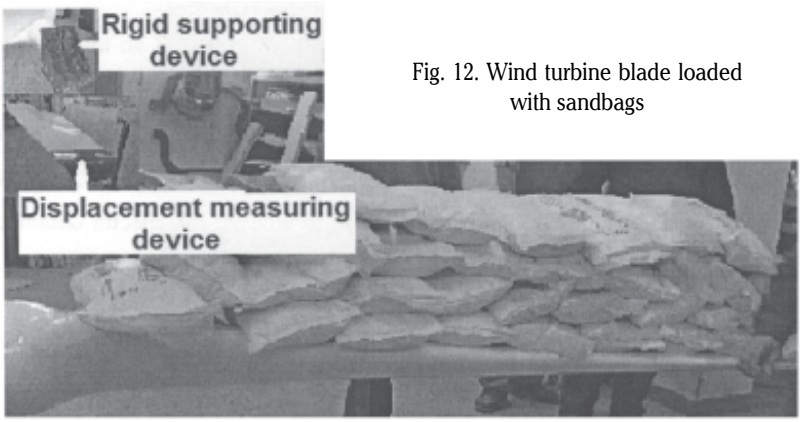

Fig. 12. Wind turbine blade loaded with sandbags

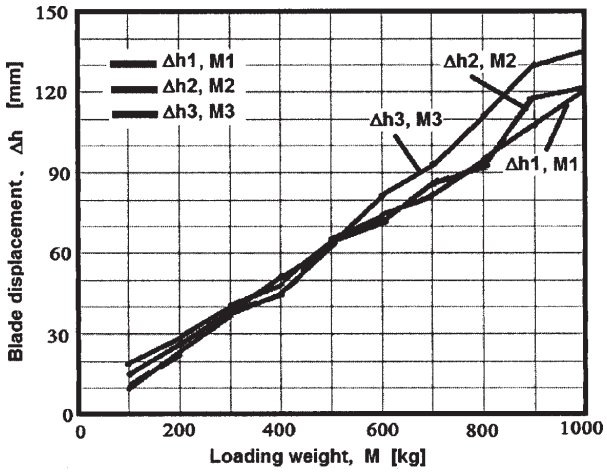

Fig. 13. The variation of blade displacement under the sandbag loading

Testing with distributed static loads on the three rotor blades

Prior to being mounted on the rotor the three blades were statically tested by distributed loading with sandbags, each one having 25 kg. For this purpose each blade was fixed in horizontal position on a rigid supporting device, (fig. 12). In order to reduce the risk of on-site blade failure, as well as, to avoid any fracture during testing (nondestructive conditions) the maximum load was limited, for the elastic deformation range of the critical section, at 50 MPa. The elastic deformation was measured on the inner side of each blade three times and step by step, measuring the displacement of the blade tip for each step of loading and unloading. The total weight required for simulating the 50 MPa stress in the critical section, was of maximum 1000 kg taking into account the presence of the metal reinforcement. This weight was approximately uniformly distributed along the blade span.

The testing results, showing the variation of the blade tip displacement under the applied load, are given graphically in figure 13. The graphic reveals a similar elastic behaviour of all three blades.

The comparison between the displacement on X axis resulted through numerical simulation of 16.86 mm with the average value obtained by the static test of about 28mm reveals a significant difference. The reason for this difference can be explained by the weight distribution of the sandbags which is not quite similar with the force given by the pressure load on the blade inner part, where the chord of the airfoil (i.e. the width of the blade) from the root and tip is very different (350 mm at the tip and 800 mm at the root). However, during the static test the blades have not been plastically deformed under load conditions which generally do not exceed the loadings generated by air flow dynamic pressure in extreme weather conditions (wind speed up to 30 m/s).

Solutions for improving the blade structure to withstand extreme weather conditions

Based on the analysis performed on the broken blade of a 5 kW wind turbine and looking further for correcting and improving the blade reliability involving design, mechanical strength and manufacturing technology, the following improving solutions are proposed:

- depending on the specific thickness prescribed for the FGRP material, the maximum number of layers (3) of fiberglass embedded in resin matrix will be used, and consequently the shell thickness of FGRP in the leading edge will be increased from 5 mm (current situation) to 15 mm;

- before gluing the two shell halves it will be strictly verified if there is a direct contact along whole gluing outline between the surfaces which have to be glued, and after gluing the two parts the blade shell will be kept in a pressing device in order the facilitate the glue to penetrate into the microstructure of the resin and particularly to bind to the fiberglass mat;

- prior to injecting the polyurethane foam, the blades have to be restrained rigidly in a device that does not allow any deformation of the FGRP shell after the foam was injected. During the curing stage the foam expands creating pressure inside the shell;

- the injection of the polyurethane foam will be performed slowly, with the blades kept in vertical position, to facilitate as much as possible a total elimination of the indoor air from the inside of the shell;

- the metal insertion must to be well glued on the two FGRP shells of the blade ensuring an effective sealing and so avoiding the moist air to penetrate inside the blade shell.

Conclusions

The study reported here reveals that structurally, as mechanical strength, the blade made of FGRP withstands the maximum loads given by extreme weather conditions (wind speeds up to 30 m/s). In areas with maximum stresses the blade mechanical strength is substantially enhanced by using metal insertion which takes over the shear force and bending moment which loads the restraint section of the blade root. Therefore, the safety factor of the blade structure complies with the values recommended by IEC 61400-2 standard. The main cause of the blade damage was the exfoliation that initially occurred at the tip of the blade caused by a poor and ineffective gluing along the jointing line, especially at the leading edge. Beside this, the presence of gaps within the polyurethane foam core had also a role. In those gaps the atmospheric moisture developed water condensation, which at negative temperatures becomes ice and expands the micro cracks and consequently weakens the blade shell material. The proposed solution for improving the blade structure will help the manufacturer to reconsider and to correct its technology avoiding other similar damages, like those described in the present paper, to happen again.

Acknowledgment: The paper is financed by Grant CNCSIS ID34/2010, EEA Grant RO-0018/2009 and Grant UEFISCDI-PCCA 36/2012.

References

1. BEJ A., Wind turbines (Turbine de vânt), Politehnica Publishing House, Timisoara, Romania, 2003, ISBN 973-625-098-9.
2. GIPE P., Wind turbine basics, Chelsea Green Publishing Company, Vermont, USA, 2009.
3. ABBOTT I. H., DOENHOFF A. E., Theory of Wing Sections, Dover Publications, Inc., New York 1958.
4. *** AutoCAD Mechanical 2010, User Guide, Autodesk Inc.
5. *** Improvement of the Structures and Efficiency of Small Horizontal Axis Wind Generators with Non-Regulated Blades, Grant RO-0018/2009.
6. *** Microgrid Integrated Small Power Renewable Energy Hybrid Systems, Grant UEFISCDI-PCCA 36/2012.
7. BEJ A., BORDEAŞU I., MILOŞ T., BĂDĂRĂU R., Mat. Plast., **49** no. 3, 2012, p. 212
8. *** ASM Handbook, vol. 21 Composites, 2001, USA, ISBN 0-87170-703-9.
9. *** IEC 61400-2/2006, Design requirements for small wind turbine, (IEC Standard)

Manuscript received: 14.10.2013